

2.1 DEVELOPMENT OF ODS FeCrAl FOR FUSION REACTOR APPLICATIONS – B. A. Pint, K. A. Unocic, S. Dryepondt and D. T. Hoelzer (Oak Ridge National Laboratory, USA)

OBJECTIVE

The dual coolant lead-lithium (DCLL) blanket concept requires improved Pb-Li compatibility with ferritic steels in order to demonstrate viable blanket operation in a DEMO-type fusion reactor. The goal of this work is to develop an oxide dispersion strengthened (ODS) alloy with improved compatibility with Pb-Li and excellent mechanical properties. The current focus is characterizing the performance of a group of ODS alloys based on Fe-12Cr-5Al.

SUMMARY

Characterization of the first four experimental ODS FeCrAl heats (based on Fe-12Cr-5Al) is nearing completion. Creep testing of the alloys containing $Y_2O_3 + ZrO_2$ and $Y_2O_3 + HfO_2$ at 800°C/100 MPa has shown exceptional lifetimes for these materials. Additional Pb-Li compatibility experiments were completed at 700°C including similar composition ODS FeCrAl alloys made for a nuclear energy project. All of the alloys showed low mass changes in these experiments, suggesting superior Pb-Li compatibility compared to wrought and ODS Fe-Cr compositions. A thin (~1 μm) reaction product of $LiAlO_2$ was observed in all cases and additional characterization is in progress. The final phase of this project will examine two new alloys made with the same Fe-12Cr-5Al powder and several new alloys where Zr was added as an alloy addition rather than an oxide dispersion.

PROGRESS AND STATUS

Introduction

The DCLL blanket concept (Pb-Li and He coolants) is the leading U.S. design for a test blanket module (TBM) for ITER and for a DEMO-type fusion reactor.[1] With reduced activation ferritic-martensitic (FM) steel as the structural material, the DCLL is limited to ~475°C metal temperature because Fe and Cr readily dissolve in Pb-Li above 500°C and Eurofer 97 plugged a Pb-Li loop at 550°C.[2-3] For a higher temperature blanket for DEMO, structural materials with enhanced creep and compatibility are needed. ODS FeCrAl alloys are one possibility to meet this objective and considerable research on ODS FeCr alloys has shown an excellent combination of creep strength and radiation resistance.[4-7] However, these ODS FeCr alloys do not have adequate compatibility with Pb-based coolants, such as Pb-Bi eutectic (LBE) [8-11]. With the addition of Al, isothermal compatibility tests have shown low mass losses at up to 800°C [12] and a recent thermal convection loop was operated for 1000h at 550°C with only small mass changes measured for the commercial Fe-21Cr-5Al-3Mo alloy (Kanthal APMT) specimens in the hot and cold legs [13]. Therefore, a materials development effort is underway, specific to this application. ODS FeCrAl was commercialized in the 1970's for its high temperature (>1000°C) creep and oxidation resistance [14] and other research groups are currently investigating new FeCrAl alloy compositions for fission and fusion applications with liquid metals [15-17].

Previous initial work [18-21] had identified Fe-12wt.%Cr-5Al as a target composition with low Cr to minimize α' formation during irradiation [22], while maintaining 5%Al for Pb-Li compatibility.[18,21] Using diffusion couples, combinations of oxides also were identified that could form stable ternary compounds. The microstructure and property assessment of this first generation of composition is nearly complete [23,24] and a second generation is being designed based on the information learned.

Experimental Procedure

Four experimental ODS FeCrAl ferritic alloys were produced by mechanical alloying (MA). Powder of specified composition Fe-12.1wt.%Cr-5.0Al and particle size range ~45-150 μm was prepared by Ar gas atomization by ATI Metal Powders. The FeCrAl powder was blended with 0.3%Y₂O₃ powder (17-31 nm crystallite size, produced by Nanophase, Inc.) and subsequent 1kg batches included additions of 0.4ZrO₂, 0.22HfO₂ and 0.2TiO₂ powders (<100 nm diameter from American Elements). Each batch was ball milled for 40 h in Ar gas atmosphere using the Zoz CM08 Simoloyer ball mill. After ball milling, the powders were placed in mild steel cans, degassed at 300°C under vacuum and sealed. The cans were equilibrated at 950°C for 1 h and then extruded through a rectangular shaped die. Table 1 shows the as-extruded compositions of each alloy. The alloys with additional ZrO₂, HfO₂ and TiO₂ oxide additions showed higher O contents and the Cr and Al contents were lower than the starting powder. Other typical impurities were Co, Cu, Ni and Mn at the 0.01-0.02% level and the C and N pickups from the milling process were acceptable. Table 1 also includes several additional alloys with higher Cr contents that were produced for a nuclear energy project. These alloys were made by a similar process but with only Y₂O₃ additions. For comparison, a commercial ODS (PM2000) and a powder metallurgy (APMT) FeCrAl alloy are shown.

Because of the relatively small amount of material fabricated, creep testing of the new alloys was performed at 800°C using 25mm long specimens parallel to the extrusion axis and with a 2 x 2 mm gauge section that was 7.6mm long. Static Pb-Li capsule tests were performed using Mo (inert to Pb-Li) inner capsules and type 304 stainless steel (SS) outer capsules to protect the inner capsule from oxidation. The ODS FeCrAl specimens were ~1.5 mm thick and 4-5 cm² in surface area with a 600 grit surface finish and were held with 1 mm diameter Mo wire. The capsules were loaded with 125 g of Pb-Li in an Ar-filled glove box. The most recent capsule tests were conducted with commercial Pb-Li from the same supplier used for the loop experiment [13]. The Mo and SS capsules were welded shut to prevent the uptake of impurities during the isothermal exposure. After exposure, residual Pb-Li on the specimen surface was removed by soaking in a 1:1:1 mixture of acetic acid, hydrogen peroxide and ethanol for up to 72 h. Mass change was measured with a Mettler-Toledo balance with an accuracy of ± 0.04 mg or 0.01 mg/cm².

Post-test specimen surfaces were examined using x-ray diffraction (XRD) and secondary electron microscopy (SEM) equipped with energy dispersive x-ray (EDX) analysis. After surface characterization, the specimens were metallographically sectioned and polished and examined by light microscopy, SEM and transmission electron microscopy (TEM). Specimens for TEM analysis were prepared by Focused Ion Beam (FIB, Hitachi model NB500) using the in-situ lift-out method. A Philips model CM200 FEG-TEM/STEM (Scanning TEM) with XEDS was used for analysis. Bright-Field (BF) and High Angle Annular Dark Field (HAADF) STEM imaging methods were used in the microstructural investigations.

Table 1. Alloy chemical compositions (mass% or ppmw) by inductively coupled plasma analysis and combustion analysis.

Material	Fe%	Cr%	Al%	Y%	O	C	N	S	Other
Powder	82.8	12.1	5.0	<	64	31	11	<3	0.004Si
125Y	83.3	11.4	4.8	0.19	842	380	455	20	0.05W, 0.02Si, 0.01Ti
125YZr	82.8	11.5	4.9	0.18	1920	250	160	10	0.30Zr, 0.01Hf, 0.01Si
125YHf	82.3	11.7	4.8	0.17	2280	220	110	10	0.68Hf, 0.01Zr, 0.01Si
125YTi	82.4	12.0	4.9	0.16	2220	350	135	30	0.20Ti, 0.01Si
134Y	82.5	12.8	4.4	0.17	1360	310	140	10	0.01Si
155YT	79.9	14.6	4.7	0.16	950	340	240	10	0.44Ti, 0.02Si
155YMT	79.0	14.6	4.8	0.16	830	370	130	<10	0.44Ti, 0.88Mo, 0.02Si
PM2000	74.1	19.1	5.5	0.39	2480	14	86	8	0.48Ti, 0.02Si
APMT	69.8	21.2	4.8	0.21	519	360	530	<3	2.8Mo, 0.1Zr, 0.2Hf, 0.5Si

< indicates below the detectability limit of <0.01%

Table 2. Measurements of the grain size and grain aspect ratio (GAR) of the ODS FeCrAl ferritic alloys.

Alloy	Grain Size (μm)		GAR (Parallel/Normal)
	Parallel to Extrusion Axis	Normal to Extrusion Axis	
125Y	0.83 ± 0.17	0.56 ± 0.09	1.48
125YZ	0.27 ± 0.06	0.17 ± 0.02	1.59
125YH	0.70 ± 0.16	0.39 ± 0.06	1.79
125YT	0.14 ± 0.02	0.12 ± 0.01	1.17

Results and Discussion

A large amount of microstructural information has been reported previously on the ODS Fe-12Cr-5Al alloys as well as aging and hardness data [20,23-25]. Table 2 summarizes the completed comparison of grain size for each of the four alloys.

Figure 1 compares the creep performance at 800°C of the ODS Fe-12Cr-5Al alloys to the commercial alloys PM2000 and APMT. Data from Plansee for fine grain (FG) PM2000 are also included. One PM2000 specimen failed during loading at 80 MPa, while an on-going 125YT test has reached 285 h with the same applied stress. For testing at 100 MPa, one 125YH specimen failed after 1242 h and one 125YZ specimen has passed 4000 h without failure. To reach a minimum lifetime of 1000h at 800°C, alloys APMT and FG PM2000 are limited to ~25 MPa and ~45 MPa, respectively. For the new 12Cr-5Al alloys, the stress can be increased to at least 80MPa. A 100MPa test is planned for 125YT and further work is needed to confirm that 125YZ exhibits the best creep properties among the new alloys.

For the Pb-Li compatibility assessment, the most recent mass change data after 1000 h at 700°C in static Pb-Li is summarized in Figure 2 with the previous result for a 125YZ specimen. In the initial set of capsule experiments under the same conditions, a 125YH specimen lost 1.3 mg/cm², but showed no visual indication of attack. A second 125YH specimen was exposed in this set of experiment and showed a low

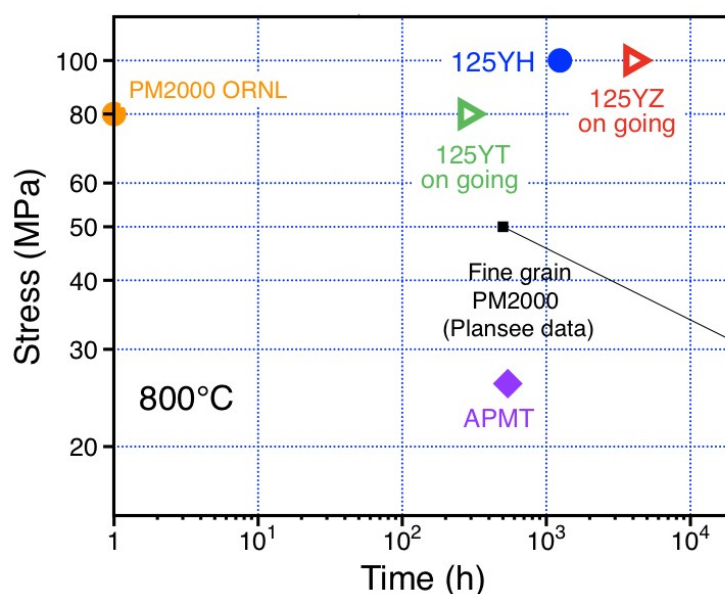


Figure 1. Lifetime at 800°C versus applied stress for the ODS Fe-12Cr-5Al, PM2000 and APMT alloys.

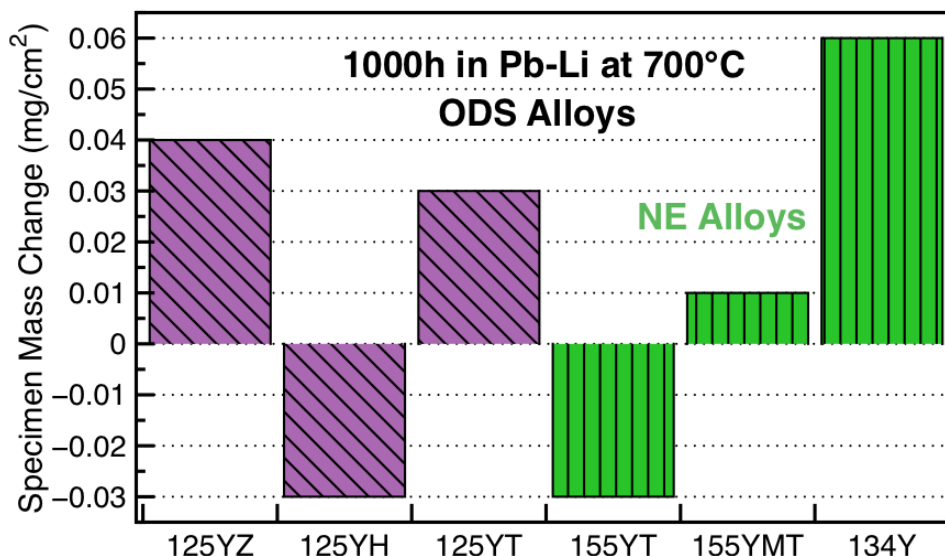


Figure 2. Specimen mass change for alloy specimens exposed for 1000h at 700°C in static Pb-Li.

mass change like the other specimens. In addition to the 12Cr-5Al specimens, ODS FeCrAl alloy specimens from another project were included that contained higher Cr contents, Table 1. These specimens also showed low mass changes after exposure and cleaning, consistent with prior work on commercial FeCrAl alloys PM2000 and APMT [12,26]. Also consistent with these prior studies, XRD identified the reaction products as LiAlO_2 in all cases. This oxide formed due to O impurities in the Pb-Li and presumably inhibited dissolution of the alloy into the liquid metal. However, the mass losses observed in the recent loop test at $\sim 450\text{-}550^\circ\text{C}$ suggest that this layer does not prevent dissolution.

Figure 3 shows cross-sections of the 12Cr-5Al ODS alloy specimens exposed in Pb-Li. In several cases, the $\sim 1\mu\text{m}$ thick LiAlO_2 layer fractured or delaminated during specimen preparation. Previously, the Al content in the alloy was measured using electronprobe microanalysis but only minor Al depletion was observed in the 125YH and 125YZ specimens [23,25]. In order to further study the reaction product, TEM cross-sections were made. Figures 4 and 5 show initial results for the 125YZ specimen. The oxide appeared to have a columnar grain structure, Figure 4. At higher magnification, voids and oxide precipitates could be observed in the LiAlO_2 layer. Voids appear light in the bright field image and dark in the HAADF image. Oxides rich in Zr should appear bright in the HAADF image and dark in the bright field image, Figure 5. The incorporation of oxides into the reaction product suggests that the layer grew by the inward transport of O, rather than outward transport of Al. Unfortunately, LiAlO_2 was easily damaged by the electron beam (as was found earlier [26]) and only limited analysis has been possible of this specimen.

In the final year of this 3-year effort, several new alloys will be briefly investigated. Two new alloys have been extruded with the same Fe-12Cr-5Al powder with additions of $\text{La}_2\text{O}_3\text{-ZrO}_2$ and $\text{Y}_2\text{O}_3\text{-Fe}_2\text{O}_3$. The former was selected to examine the oxide precipitates formed in the alloy with La rather than Y and the latter was made to replace the 125Y alloy baseline alloy that had a lower O content than the other alloys (Table 1) and was contaminated with Fe-Cr powder resulting in questionable mechanical properties and Pb-Li compatibility [25]. In addition, new powder was ordered with Fe-12Cr-5.6Al and Fe-10Cr-6Al base compositions and alloys additions of Zr, Hf or Zr and Ti. The primary goal with these powders is to determine if different oxides form if, for example, the Zr is added as an alloy addition rather than as ZrO_2 .

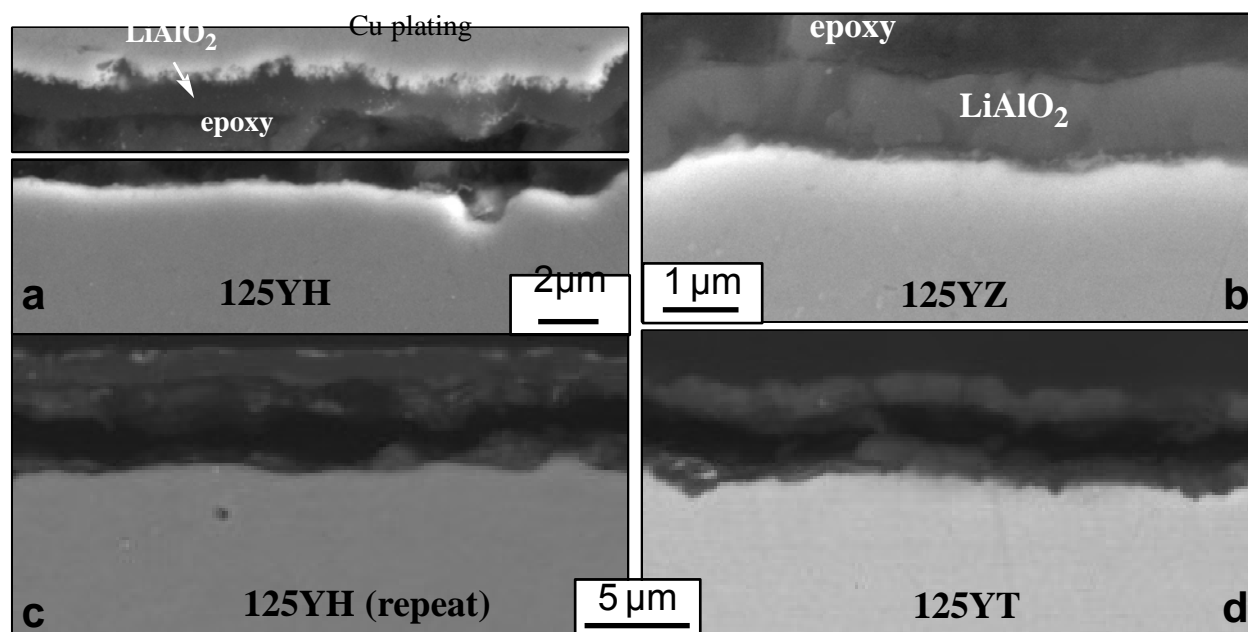


Figure 3. SEM backscattered electron images of polished cross-sections after 1000 h in Pb-Li at 700°C of (a) 125YH, (b) 125YZ, (c) 2nd 125YH specimen and (d) 125YT. In (a), (c) and (d) the oxide delaminated during specimen preparation.

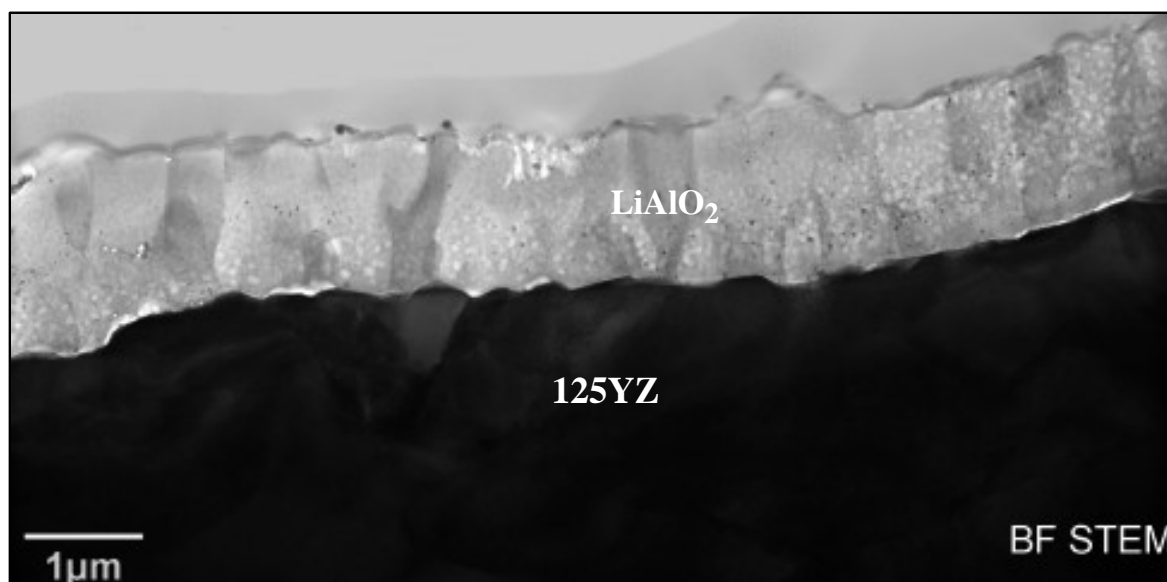


Figure 4. Bright field STEM image of the oxide formed on 125YZ after 1000h at 700°C in PbLi.

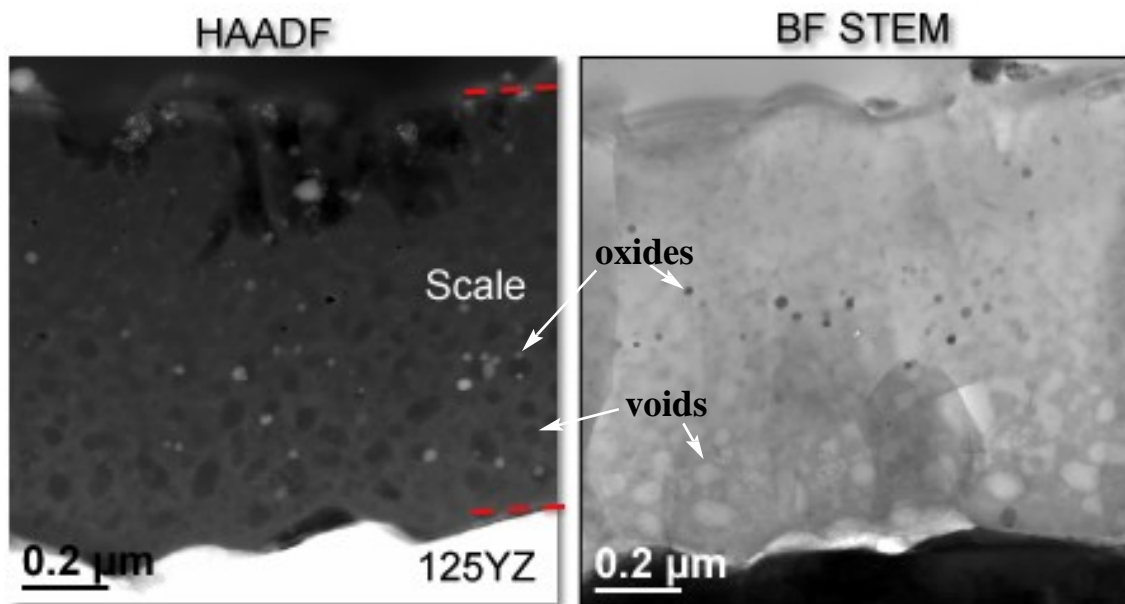


Figure 5. STEM cross-sectional images of the oxide formed on 125YZ after 1000h at 700°C in PbLi.

References

- [1] M. Abdou, D. Sze, C. Wong, M. Sawan, A. Ying, N. B. Morley and S. Malang, *Fus. Sci. Tech.*, 47 (2005) 475.
- [2] O. K. Chopra, D. L. Smith, P. F. Tortorelli, J. H. DeVan and D. K. Sze, *Fusion Technol.*, 8 (1985) 1956.
- [3] J. Konys, W. Krauss, J. Novotny, H. Steiner, Z. Voss and O. Wedemeyer, *J. Nucl. Mater.* 386-88 (2009) 678.
- [4] S. Ukai and M. Fujiwara, *J. Nucl. Mater.* 307 (2002) 749.
- [5] G. R. Romanowski, L. L. Snead, R. L. Klueh, D. T. Hoelzer, *J. Nucl. Mater.*, 283-287 (2000) 642.
- [6] R. L. Klueh, J. P. Shingledecker, R. W. Swindeman, D. T. Hoelzer, *J. Nucl. Mater.* 341 (2005) 103.
- [7] D. A. McClintock, M. A. Sokolov, D. T. Hoelzer and R. K. Nanstad, *J. Nucl. Mater.*, 392 (2009) 353.
- [8] T. Furukawa, G. Müller, G. Schumacher, A. Weisenburger, A. Heinzl and K. Aoto, *J. Nucl. Mater.* 335 (2004), 189.
- [9] P. Hosemann, H.T. Thau, A.L. Johnson, S.A. Maloy and N. Li, *J. Nucl. Mater.* 373 (2008) 246.
- [10] C. Schroer, J. Konys, T. Furukawa and K. Aoto, *J. Nucl. Mater.* 398 (2010) 109.
- [11] A. Weisenburger, K. Aoto, G. Müller, A. Heinzl, G. Schumacher and T. Furukawa, *J. Nucl. Mater.* 358 (2006) 69.
- [12] B. A. Pint, L. R. Walker and K. A. Unocic, *Mater. High Temp.* 29 (2012) 129.
- [13] S. J. Pawel, DOE/ER-0313/56 (2014) 178.
- [14] J. D. Whittenberger, *Met. Trans.* 9A (1978) 101.
- [15] J. Lim, H.O. Nam, I.S. Hwang and J.H. Kim, *J. Nucl. Mater.* 407 (2010) 205.
- [16] A. Kimura, et al., *J. Nucl. Mater.* 417 (2011) 176.
- [17] S. Takaya, et al., *J. Nucl. Mater.* 428 (2012) 125.
- [18] B. A. Pint, D. T. Hoelzer, D. Shin, J. O. Kiggans, Jr., K. A. Unocic, DOE/ER-0313/53 (2012) 10.
- [19] B. A. Pint, D. T. Hoelzer and K. A. Unocic, DOE/ER-0313/54 (2013) 27.
- [20] D. T. Hoelzer, K. A. Unocic, S. Dryepondt and B. A. Pint, DOE/ER-0313/55 (2013) 5.
- [21] K. A. Unocic and B. A. Pint, *J. Nucl. Mater.* 455 (2014) 330.

- [22] C. Capdevila, M.K. Miller, K.F. Russell, J. Chao, J.L. González-Carrasco, *Mater. Sci. Eng. A* 490 (2008), 277.
- [23] B. A. Pint, S. Dryepondt, K. A. Unocic and D. T. Hoelzer, *JOM* 66 (2014) 2458.
- [24] K. A. Unocic, D. T. Hoelzer and B. A. Pint, *Mater. High Temp.* 32 (2015) 123.
- [25] B. A. Pint, K. A. Unocic, S. Dryepondt and D. T. Hoelzer DOE-ER-0313/56 (2014) 31.
- [26] B. A. Pint and K. L. More, *J. Nucl. Mater.* 376 (2008) 108.